http://dx.doi.org/10.5012/bkcs.2013.34.6.1771

Calculation of Potential Energy Curves of Excited States of Molecular Hydrogen by Multi-Reference Configuration-interaction Method

Chun-Woo Lee,* Yeongrok Gim, and Tae Hoon Choi†

*Department of Chemistry, Ajou University, Woncheon-Dong, Yeongtong-Gu, Suwon 443-749, Korea. *E-mail: clee@ajou.ac.kr*
†Department of Chemical Engineering Education, Chungnam National University, Daejeon 305-764, Korea
Received February 19, 2013, Accepted March 20, 2013

For the excited states of a hydrogen molecule up to $n = 3$ active spaces, potential energy curves (PECs) are obtained for values of the internuclear distance R in the interval [0.5, 10] a.u. within an accuracy of 1×10^{-4} a.u. (Hartree) compared to the accurate PECs of Kolos, Wolniewicz, and their collaborators by using the multi-reference configuration-interaction method and Kaufmann's Rydberg basis functions. It is found that the accuracy of the PECs can be further improved beyond 1×10^{-4} a.u. for that R interval by including the Rydberg basis functions with angular momentum quantum numbers higher than $l = 4$.

Key Words : Potential energy curves, Excited Rydberg states, Multi-reference CI

Introduction

To calculate the photoabsorption and photoionization spectra of molecules, one needs to know the potential energy surfaces of the dipole-allowed states. In particular, the potential energy surfaces of the Rydberg states are the basic input for calculating the photoionization by multichannel quantum defect theory (MQDT).[1] Modern electronic structure theory is believed to be able to calculate the potential energy surfaces for the excited states, including Rydberg states, with chemical accuracy. However, the degree of accuracy, excitation region, and types of application differ from problem to problem. Thus, depending on the problem, different physical situations and accordingly different types of demands prevail. In particular, to calculate the photoionization spectra, the shape of the potentials in the neighborhood of the equilibrium positions is not enough. One needs to know the accurate potential energy surfaces over the range of internuclear distances that contribute to the Franck–Condon factor. In this case, information on the spectroscopic constants is not enough to test the accuracy of the calculated potentials. For diatomic molecules, the experimentally determined Rydberg–Klein–Rees (RKR)[2] potential energy curves (PECs) provide valuable information for testing the calculated potentials. The RKR PECs, however, are not always consistent and are valid only within the framework of the semi-classical theory.

For the H_2 molecule, there is a better way of judging the accuracy of the calculated PECs: using the highly accurate potentials of Kolos, Wolniewicz, and their collaborators,[3-12] which were obtained by using a large number of trial functions containing r_{12} terms. Their PECs are shown in Figure 1. Thus, we use their PECs to evaluate the accuracy of the PECs obtained by modern electronic structure methods. The multi-reference configuration-interaction (MRCI) method,[13] complete active space second-order perturbation (CASPT2) method,[14] equation of motion coupled-cluster singles and doubles (EOM-CCSD) method,[15] and time-dependent density functional theory can be used to obtain the potential energy surfaces for excited states. Among these methods, MRCI is known to always yield reliable potentials and thus was chosen for this study. Calculations of the potentials for excited states frequently suffer from the root-flipping problem and pose a great difficulty. In MRCI, this problem can be overcome by judicious choices of the values of parameters such as the size of the active space and primary space[16] and the number of correlated multi-configurational self-consistent field (MCSCF) reference functions.[17,18]

Preliminary calculation of the dipole-allowed states of nitrogen molecules shows that it is very hard to obtain good PECs for Rydberg states without including the Rydberg basis functions. Dunning devised Rydberg basis functions for the Rydberg states of the first-row atoms.[19] Unfortunate-

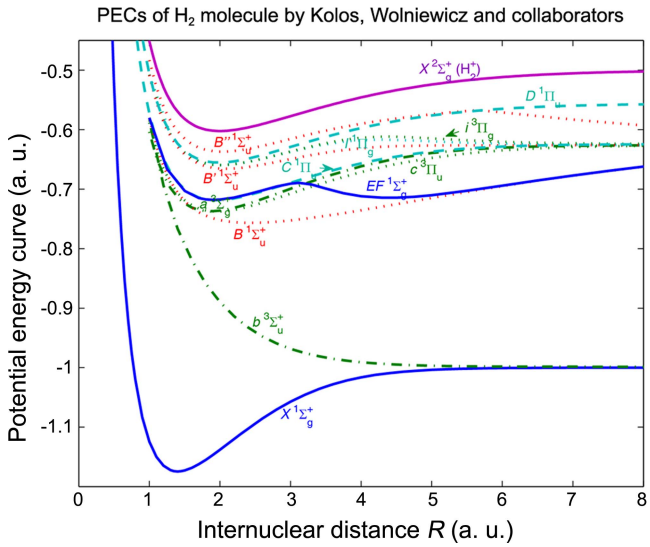

Figure 1. Potential energy curves of H_2 obtained by Kolos, Wolniewicz, and their collaborators using the method containing r_{12} terms.[3-12]

ly, he did not devise Rydberg functions for the hydrogen atom. The other option is to use a universal Gaussian basis set devised by Kaufmann. It is used to construct the Rydberg natural basis set in the method devised by Roos and his collaborators[20] and implemented in MOLCAS. Because MOLCAS is not available to us, we decided to simply use Kaufmann's Rydberg basis functions[21] without processing, as is done in MOLCAS, and examine what physics is involved in the use of these Rydberg basis functions, how much the PECs are improved by including the Rydberg basis functions, what factor is the most important for obtaining the best PECs, and what is the most efficient way of using Rydberg basis functions.

We used the MRCI method in the Molpro package.[22] It combines the MCSCF method of Werner, Meyer, and Knowles[16,23] and the internally contracted self-consistent electron pair theory[24] for the multi-reference configuration interaction method, which greatly simplifies the matrix operation in Roo's direct configuration interaction method.[25]

Potential Energy Curves for the States with $n = 2$ Complete Active Space. States that decompose into H(1s) + H(1s) and H(1s) + H(2l) are expected to have PECs that can be calculated within the complete active space (CAS) for n = 1 and 2, which consists of $(3\sigma_g^+,1\pi_u,3\sigma_u^+,1\pi_g)$. States $X^1\Sigma_g^+$, $b^3\Sigma_u^+$, $B^1\Sigma_u^+$, $E,F^1\Sigma_g^+$, $c^3\Pi_u$, $a^3\Sigma_g^+$, $C^1\Pi_u$, $l^1\Pi_g$, $i^3\Pi_g$, $e^3\Sigma_u^+$, $B'^1\Sigma_u^+$, $h^3\Sigma_g^+$, and $m^3\Sigma_u^+$ correlate to H(1s) + H(1s) and H(1s) + H(2l). Among these, we calculated PECs for $X^1\Sigma_g^+$, $b^3\Sigma_u^+$, $B^1\Sigma_u^+$, $E,F^1\Sigma_g^+$, $a^3\Sigma_g^+$, and $C^1\Pi_u$ which are the first states in their own symmetries except for $E,F^1\Sigma_g^+$. The calculations for the first states are usually easier and more accurate because there is no state to which orthogonalization is applied according to the variation principle. PECs obtained with the correlation-consistent basis set aug-cc-pVQZ (AVQZ)[26] in the CAS consisting of $(3\sigma_g^+,1\pi_u,3\sigma_u^+,1\pi_g)$ are shown in Figure 2 with the corresponding accurate PECs obtained by Kolos, Wolniewicz, and their collaborators.[3-12]

Most of the PECs calculated by MRCI[13,18,24,27] exhibit excellent agreement with those obtained by Kolos, Wolniewicz, and their collaborators. For the $b^3\Sigma_u^+$ state, the PEC calculated by MRCI is lower than that of Kolos and Wolniewicz,[3] indicating that not enough terms are included in Kolos and Wolniewicz's calculation. For the $a^3\Sigma_g^+$ state, the agreement between the PECs from MRCI and those obtained by Kolos and Wolniewicz[5] is excellent at R smaller than ~3 a.u., but a difference can be distinguished at R larger than ~3 a.u. For the $E,F^1\Sigma_g^+$ state,[6] the difference between the two PECs can be discerned in the range between the first minimum and the hump. The disagreement between the two PECs in the $E,F^1\Sigma_g^+$ state can be removed by increasing the size of the basis set from AVQZ to AV6Z. On the other hand, the difference in PECs for the $a^3\Sigma_g^+$ state at large r cannot be removed by increasing the size of the basis set. To remove the difference, we have to add high-angular-momentum Rydberg basis functions as high as l = 4, which will be discussed in a later section. Calculation shows that an increase in the size of the active space from $(3\sigma_g^+,1\pi_u,3\sigma_u^+,1\pi_g)$ to $(5\sigma_g^+,1\pi_u,5\sigma_u^+,2\pi_g)$ yields values of PECs that differ only at the eighth significant number.

Potential Energy Curves for Dipole-Allowed States. Let us consider the PECs for the dipole-allowed states $B^1\Sigma_u^+$, $B'^1\Sigma_u^+$, $B''^1\Sigma_u^+$, $C^1\Pi_u$, and $D^1\Pi_u$ from $X^1\Sigma_g^+$, which are important in the study of photoabsorption and photoionization. First, let us consider the PECs for the $B^1\Sigma_u^+$, $B'^1\Sigma_u^+$, and $B''^1\Sigma_u^+$ states. The $B^1\Sigma_u^+$ and $B'^1\Sigma_u^+$ states decompose into H(1s) + H(2l), and the $B''^1\Sigma_u^+$ state decomposes into H(1s) + H(3l). The difficulty caused by root flipping can be avoided in calculation by the MCSCF method by optimizing the energy average of states[28] whose number is taken to be larger than the number of states in which we are interested. For this calculation to be meaningful, the active space should be taken as large as $(5\sigma_g^+,2\pi_u,5\sigma_u^+,2\pi_g)$ owing to the presence of the $B''^1\Sigma_u^+$ state. Figure 3 shows that the PEC for

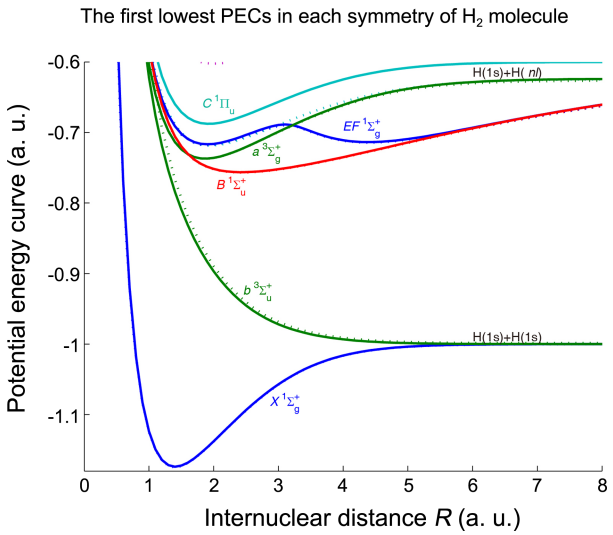

Figure 2. Potential energy curves for selected states whose active spaces are given by $(3\sigma_g^+,1\pi_u,3\sigma_u^+,1\pi_g)$. Solid lines indicate potentials obtained in this work; dotted lines indicate those of Kolos, Wolniewicz, and their collaborators.[3-12]

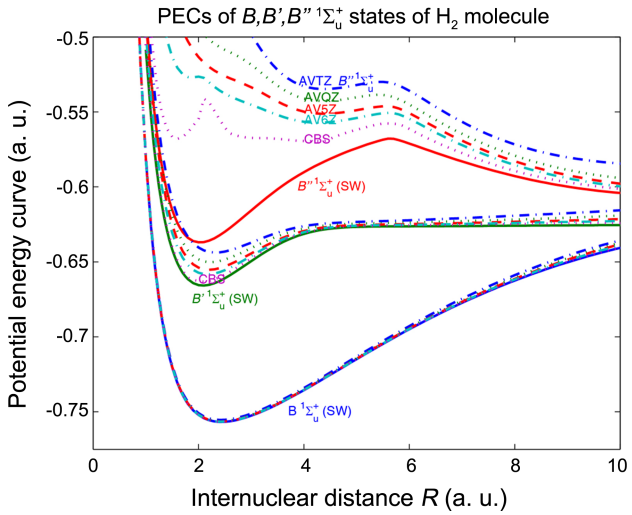

Figure 3. Comparison of potential energy curves of the dipole-allowed states $B,B',B''^1\Sigma_u^+$ obtained from MRCI with the accurate ones of Staszewska and Wolniewicz.[11] See text for details.

$B^1\Sigma_u^+$ agrees with that of Staszewska and Wolniewicz[11] with the size of the basis set equal to aug-cc-pV5Z (≡ AV5Z) or larger at R smaller than ~7 a.u. but exhibits increasing deviation as R increases. The difference becomes zero at the complete basis set (CBS) limit obtained by using the extrapolation formulas for the Hartree–Fock reference and correlation energies as follows:[22]

$$E_{HF}(n) = E_{HF}(CBS) + A \exp(-Cn)$$
$$E_{corr}(n) = E_{corr}(CBS) + A \exp(-(n-1)) + B \exp(-(n-1)^2)$$
$$E(n) = E_{HF}(n) + E_{corr}(n) \quad (1)$$

where n = 3, 4, 5, 6, …, ∞ for aug-cc-pVXZ (≡ AVXZ) with X = T, Q, 5, 6, …, ∞, respectively. For $B'^1\Sigma_u^+$, the PEC obtained from MRCI deviates greatly from that of Staszewska and Wolniewicz.[11] The difference is clearly visible even at the CBS limit obtained by using Eq. (1). For $B''^1\Sigma_u^+$, the MRCI method with AVXZ basis sets completely fails.

Because $B'^1\Sigma_u^+$ and $B''^1\Sigma_u^+$ are Rydberg states, AVXZ may be fundamentally incapable of dealing with these states because the basis set is optimized for the valence states. To treat the Rydberg states properly, this basis set should be augmented with the Rydberg basis functions. Before considering the Rydberg basis functions, let us just show in Figure 4 the same type of calculation for another type of dipole-allowed state, $C^1\Pi_u$ and $D^1\Pi_u$.

The figure tells us that, for this symmetry, the situation becomes worse, and even the first state, $C^1\Pi_u$, cannot be described with AVXZ (X = D, T, Q, 5, 6). One may claim that the failure to obtain correct PECs may be due to the failure in the MRCI method rather than to the basis set. This possibility can be tested by trying to use other methods. EOM-CCSD and CASPT2 were used to obtained the PECs, and both yielded almost the same PECs as MRCI. This means that the failure does not arise from the method employed. Because highly excited states are expected to be of the Rydberg type, the inadequacy of the basis set AVXZ

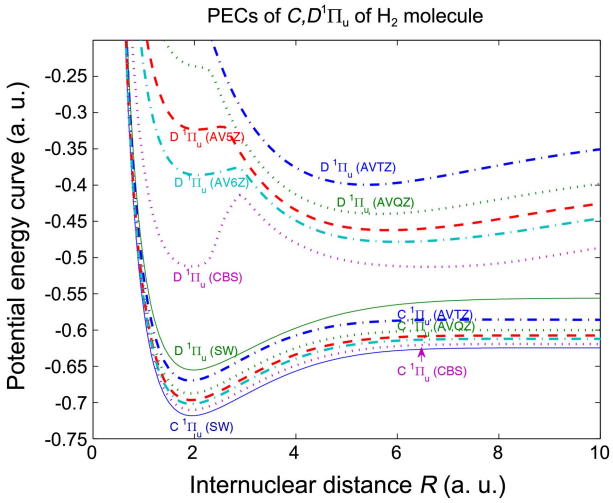

Figure 4. Comparison of potential energy curves of the dipole-allowed states $C, D^1\Pi_u$ obtained from MRCI with the accurate ones of Staszewska and Wolniewicz.[11] See text for details.

(X = D, T, Q, 5, 6) for the representation of Rydberg states may be the most likely cause of this failure.

Calculations Including Rydberg Basis Sets. Numerous studies have attempted to obtain the potential energy surfaces for Rydberg molecular states. Those studies can be grouped into two types. One type uses the effective potentials,[29] and the other introduces new basis sets for Rydberg orbitals. Using the latter approach, Lefevbre-Brion and her collaborators used several sets of Slater Rydberg basis sets using the orbital exponents obtained by the Slater rule.[30] Dunning considered augmentation of the (9s5p) basis sets with diffuse functions. Single s, p, and d exponents were obtained for the n = 3 and 4 Rydberg states of the first-row atoms.[19] He also obtained double-zeta-type Rydberg basis functions by introducing splitting factors for converting the single exponents into two exponents. The orbital exponents optimized by Dunning can be found at the EMSL basis set exchange website.[19] They were obtained for the (9s5p) basis sets but can be used with other valence basis sets.[31] The most extensive studies of Rydberg basis sets may be those by Roos and his collaborators.[32] Their method generates the atomic natural orbitals in situ for each target molecule from the universal Gaussian Rydberg basis set devised by Kaufmann[21] and uses them as the Rydberg basis sets. Their method is implemented in MOLCAS. In this study, we decided simply to use Kaufmann's Gaussian Rydberg basis set itself without processing it into a natural basis set. We felt that many points regarding the choice and use of Rydberg basis sets are unclear in the literature and thereby need to be explored further for problems where accurate energy curves are available. The hydrogen molecule is such a system and may have an advantage in that Kaufmann's basis set can be used without further processing.

Kaufmann considered the problem of obtaining a single Gaussian orbital exponent that maximizes the overlap of the Gaussian-type function with a given Slater-type orbital function. From this study, he obtained the universal Gaussian orbital exponents shown in Table 1, which can be used for all neutral molecules. The contracted Gaussian basis set using theses exponents forms a Rydberg basis set. Let us first use only the s-, p-, and d-type Rydberg basis functions, as in MOLCAS.

(s, p, d) Rydberg Basis Set: This Rydberg basis set composed of s-, p-, and d-types either can be applied to

Table 1. Exponents used for the Rydberg orbitals for molecules[21]

s-type	p-type	d-type	f-type	g-type
0.024624	0.042335	0.06054	0.07907	0.097827
0.011253	0.019254	0.027446	0.035763	0.044169
0.005858	0.009988	0.014204	0.018478	0.022792
0.003346	0.005689	0.008077	0.010493	0.01293
0.002048	0.003476	0.004927	0.006395	0.007874
0.001324	0.002242	0.003175	0.004117	0.005067
0.000893	0.001511	0.002137	0.00277	0.003407
0.000624	0.001055	0.001491	0.001931	0.002374

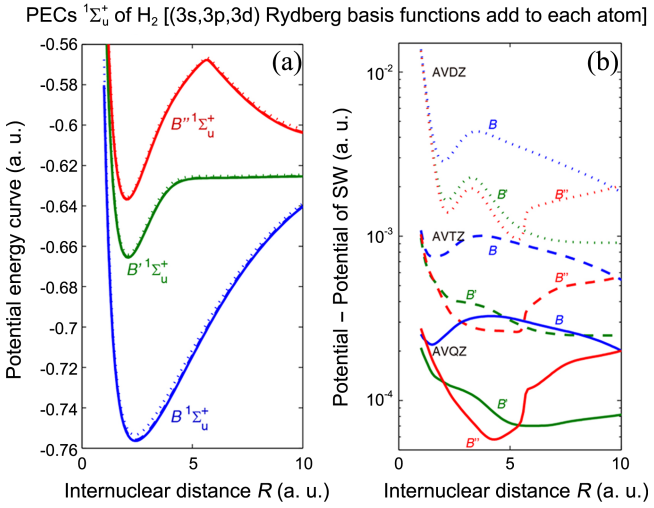

Figure 5. (a) Potential energy curves and (b) their deviations from the corresponding accurate ones of Staszewska and Wolniewicz (SW) for the dipole-allowed states $B,B',B''\,^1\Sigma_u^+$ obtained from MRCI with (3s, 3p, 3d) Rydberg functions located at each nucleus. The same line patterns and colors are used in both (a) and (b) and also in Figs. 6-9.

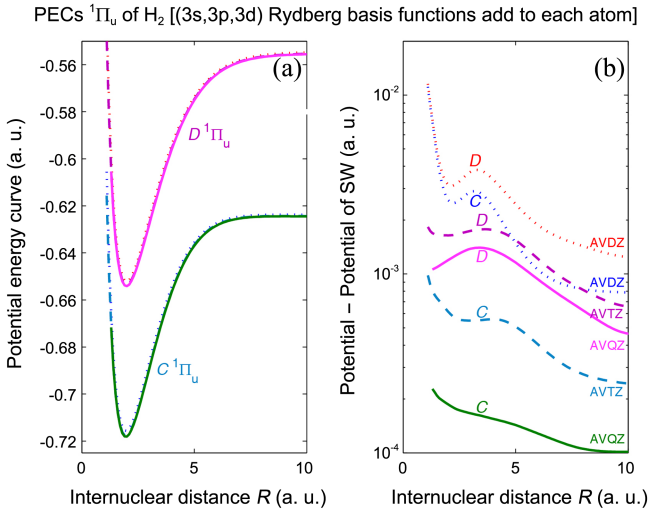

Figure 6. (a) Potential energy curves and (b) their deviations from the corresponding accurate ones of Staszewska and Wolniewicz (SW) for the dipole-allowed states $C, D\,^1\Pi_u$ obtained from MRCI with (3s, 3p, 3d) Rydberg functions located at each nucleus.

molecules by augmenting the valence basis set of each atom in molecules with this set, or by considering the single set of this Rydberg basis function located at the molecular center of charge. Dunning's Rydberg basis function is designed to be used in the former way; MOLCAS adopts the latter. We will test both ways by applying these Rydberg basis functions to the PECs for the dipole-allowed states of a hydrogen molecule considered in the previous section.

Figure 5 compares the PECs of $B\,^1\Sigma_u^+$, $B'\,^1\Sigma_u^+$, and $B''\,^1\Sigma_u^+$ obtained by Staszewska and Wolniewicz[11] and those obtained from MRCI with three Rydberg basis functions for each s-, p-, and d-type added to the valence basis sets AVDZ, AVTZ, and AVQZ for each hydrogen atom: AVXZ + (3s, 3p, 3d). Since Rydberg orbitals are basically the same as the orbitals of a hydrogen atom, usually the same numbers are used for all types as a balenced set. The comparison shows that the PECs calculated in the basis set AVDZ augmented with (3s, 3p, 3d) Rydberg basis functions are much better than those in Figure 3. Now all three PECs behave correctly for values of the internuclear distance R in the interval [0.5,10] a.u. and show minor deviation from the accurate PECs of Staszewska and Wolniewicz. Although greatly improved, they still differ from the accurate ones. Interestingly, the poorest result is obtained for the $B\,^1\Sigma_u^+$ state, for which the previous calculation without Rydberg basis functions yielded the best results. However, the error in $B\,^1\Sigma_u^+$ is still not very big and can be reduced to $0.5–1 \times 10^{-3}$ a.u. with AVTZ. The error becomes as small as $2–3 \times 10^{-4}$ a.u. and thus can be negligible when AVQZ is used.

In the difference graph for B, the error decreases at first but rebounds at $R \sim 1.5$ a.u. (AVTZ, AVQZ) as R increases. After reaching a maximum at $R \sim 3.5$ (AVTZ) or ~4.2 a.u. (AVQZ), it decreases monotonically. For B', a shoulder appears instead of the minimum, and the error rebounds at ~8 a.u. (AVTZ) or ~6 a.u. (AVQZ) instead of exhibiting a monotonic decrease. For B'', the error suddenly increases greatly at $R \sim 5.6$ a.u. owing to the perturbation from an intruder.

Figure 6 shows a comparison similar to that in Figure 5 for $C\,^1\Pi_u$ and $D\,^1\Pi_u$. The comparison shows that the PECS are also greatly improved compared with those in Figure 4 by the augmentation of the valence basis set with (3s, 3p, 3d) Rydberg basis functions, as in Figure 5, but still differ from the accurate PECs of Staszewska and Wolniewicz. The difference almost disappears (1–1.1 × 10^{-4} a.u.) for the $C\,^1\Pi_u$ state when the basis sets are enlarged to AVQZ. For the $D\,^1\Pi_u$ state, however, a difference larger than 10^{-3} a.u. from the accurate one around $R \sim 3$ a.u. can still be seen even with the large AVQZ set, in contrast to the result in Figure 5, where fair agreement ($< 2.5 \times 10^{-4}$ a.u.) is obtained for all states $B\,^1\Sigma_u^+$, $B'\,^1\Sigma_u^+$, and $B''\,^1\Sigma_u^+$. The figure shows that the discrepancy tends to decrease as the internuclear distance R increases. The tendency in the difference graph is similar to that for the $^1\Sigma_u^+$ symmetry. There is a maximum at $R \sim 3.5$ a.u. for D and a maximum (R ~ 4 a.u.) or shoulder ($R \sim 3$ a.u.) for C. After the maximum or shoulder, the error decreases monotonically as R increases.

Now, let us consider the PECs obtained with the Rydberg basis functions located at the molecular center of charge. The basis set is taken to be composed of (8s, 8p, 8d) Rydberg functions. If the set of (3s, 3p, 3d) Rydberg functions is used instead of (8s, 8p, 8d), as in the preceding case of locating Rydberg functions on each nucleus, a much worse result is obtained than that for the preceding case. Roughly speaking, twice as many Rydberg basis functions, *i.e.*, (6s, 6p, 6d), should be used to obtain the same level of accuracy as in the preceding case. For the diatomic molecule, this rule amounts to the same number of Rydberg basis functions being used for both ways. Here, the (8s, 8p, 8d) basis set is used to get a slightly better result. Let us first consider the

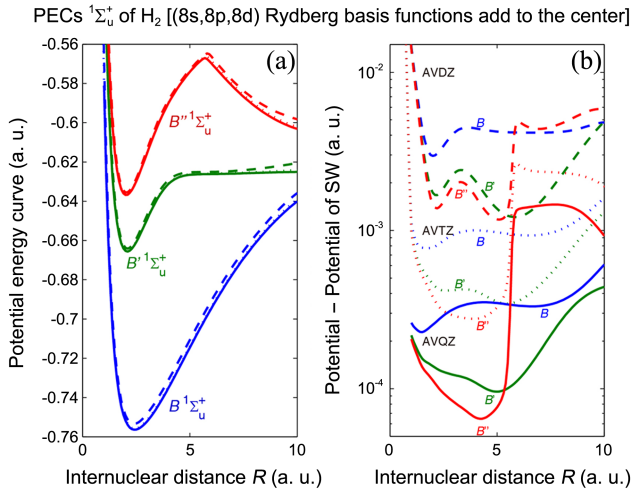

Figure 7. (a) Potential energy curves and (b) their deviations from the corresponding accurate ones of Staszewska and Wolniewicz (SW) for the dipole-allowed states $B,B',B''\,^1\Sigma_u^+$ obtained from MRCI with AVDZ, AVTZ, and AVQZ augmented with (8s, 8p, 8d) Rydberg functions located at the molecular center of charge.

$^1\Sigma_u^+$ symmetry.

The difference graph in Figure 7 shows the same trends as those in Figure 5 at $R < 5$ a.u. However, different trends appear at large R. Now, instead of decreasing, the error is amplified at large R. Figure 8 shows the results for the PECs of $^1\Pi_u$ symmetry obtained with the (8s, 8p, 8d) Rydberg basis functions located at the molecular center of charge. It shows trends similar to those seen in Figure 7 for $^1\Sigma_u^+$ symmetry. That is, instead of decreasing, the difference is amplified at large R. For AVTZ and AVQZ, the trends in the difference graph are very simple. The errors in the PECs first decrease and then increase after reaching minima at $R \sim 2.5$ a.u. (C) and ~ 3.2 a.u. (D). Although it seems unpromising, this way of using the Rydberg basis functions offers one

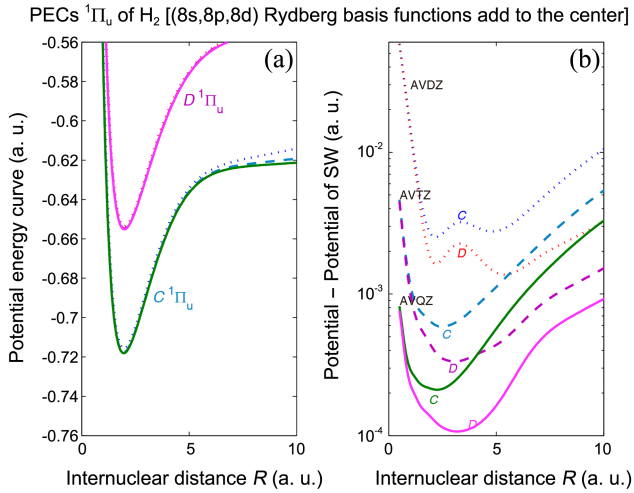

Figure 8. (a) Potential energy curves and (b) their deviations from the corresponding accurate ones of Staszewska and Wolniewicz (SW) for the dipole-allowed states $C, D\,^1\Pi_u$ obtained from MRCI with AVDZ, AVTZ, and AVQZ augmented with (8s, 8p, 8d) Rydberg functions located at the molecular center of charge.

advantage. Namely, Figure 8(b) shows that the error for $D^1\Pi_u$ is now smaller than that for $C^1\Pi_u$, in great contrast to the unacceptably large error for $D^1\Pi_u$ in Figure 6.

The results obtained so far can be summarized as follows. Without the inclusion of the Rydberg basis functions, the PECs obtained with valence basis sets alone for the $B''\,^1\Sigma_u^+$ and $D^1\Pi_u$ states from MRCI are completely absurd even in the CBS limits. Better PECs for the lower states $B'\,^1\Sigma_u^+$ and $C^1\Pi_u$ are obtained but still do not converge to the PECs of Staszewska and Wolniewicz at the CBS limit. With the basis set augmented with Rydberg functions for each atom, very excellent PECs are obtained for the states belonging to the symmetry $^1\Sigma_u^+$. Similarly, an excellent PEC is obtained for the first state of symmetry $^1\Pi_u$ by using the basis set augmented with Rydberg basis functions for each atom. However, the error in the PEC for $D^1\Pi_u$ is larger than 10^{-3} a.u. at $0 < R < 5.5$ a.u. and appears problematic because the range of bad behavior is a physically important range. When the different method of locating the Rydberg basis functions at the molecular center of charge is employed, the problem of the PEC for $D^1\Pi_u$ at $0 < R < 5.5$ a.u. disappears, although a new problem appears at large R. That is, the PEC begins to deviate increasingly from the correct PEC as the internuclear distance increases. This undesirable behavior at large R also holds for $C^1\Pi_u$.

This phenomenon is easily understood if we recognize that molecules become atom-like at smaller internuclear distances, at which the electronic states become more like Rydberg states located at the molecular center of charge. Mulliken called this phenomenon Rydbergization.[33] Molecular states become more like Rydberg states as n increases, which explains why $D^1\Pi_u$ is well described at $0 < R < 5.5$ a.u. by the Rydberg basis functions located at the molecular center of charge. At large internuclear distances, the shape of a molecule differs greatly from that of an atom, and the Rydberg basis functions located at the molecular center of charge yield a poor result at large R. The reverse will be true when Rydberg basis functions are added to the valence basis sets.

The Importance of the High-Angular-Momentum Rydberg Basis Set: Consider an approach in which Rydberg basis functions are located on each nucleus. If (2s, 2p, 2d) Rydberg basis functions are used, the quality of PECs of $^1\Sigma_u^+$ symmetry obtained from MRCI is generally good except for B''. The discrepancy in B'' disappears when (3s, 3p, 3d) Rydberg basis functions are used. The quality of PECs of $^1\Pi_u$ symmetry is good for C; however, it is good only at large R for D and exhibits problems at small and intermediate R. Presumably, better agreement would be obtained by using the (4s, 4p, 4d) Rydberg set. However, this Rydberg set cannot be used because of the numerical instability caused by the very small overlap arising from the too-wide range of orbital exponents. This error in D cannot be removed by locating Rydberg functions on each nucleus.

If Rydberg basis functions located at the molecular center of charge are used, more Rydberg basis functions can be added without causing a numerical problem. This way of

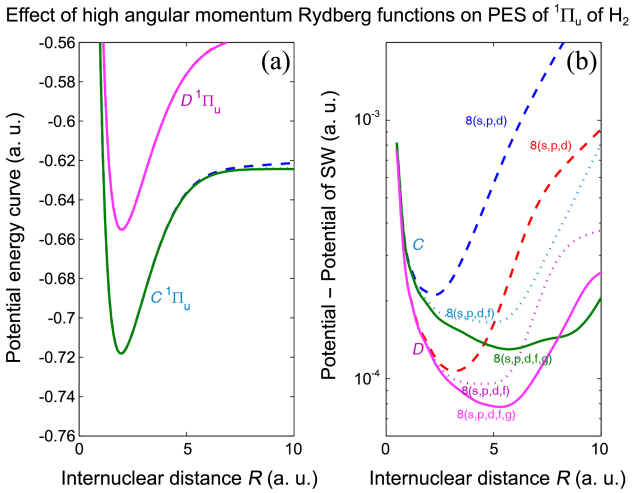

Figure 9. (a) Potential energy curves and (b) their deviations from the corresponding accurate ones of Staszewska and Wolniewicz (SW) for the dipole-allowed states $C, D\,^1\Pi_u$ obtained from MRCI with AVQZ and stepwise-extended (8s, 8p, 8d), (8s, 8p, 8d, 8f), and (8s, 8p, 8d, 8f, 8g) Rydberg functions located at the molecular center of charge.

using Rydberg functions strictly follows the definition of Rydberg orbitals and is thus physically more pleasing. This method, however, yields rather poor PECs at large R. The problem is more pronounced for $^1\Pi_u$ symmetry. The problem arises because the electronic state becomes more anisotropic as R becomes large, so it cannot be represented in terms of s-, p-, and d-type basis functions only. This argument suggests that the use of basis functions of larger angular momentum quantum number will greatly improve the PECs at large R.

The effect of higher-angular-momentum Rydberg basis functions is examined in Figure 9 with additional (8s, 8p, 8d, 8f) and (8s, 8p, 8d, 8f, 8g) Rydberg sets. It shows that the deviation of the PECs from the accurate ones at large R begins to disappear with the inclusion of f and g Rydberg basis functions. Greater improvement occurs for the $C\,^1\Pi_u$ state than for the $D\,^1\Pi_u$ state. With the (8s, 8p, 8d, 8f, 8g) Rydberg basis set and AVQZ for the valence shell, the difference between the obtained PECs and the accurate ones is smaller than 2.5×10^{-4} for R values in the interval [0,10] a.u. The error becomes larger as R increases at $R > 6$ a.u. This increase suggests that a better potential would be obtained if Rydberg functions with larger than 4 are included.

The (8s, 8p, 8d, 8f, 8g) set seems too big. Further calculation shows that a smaller (4s, 4p, 4d, 3f, 3g) Rydberg basis set differs by no more than 10^{-4} a.u. from the result for the (8s, 8p, 8d, 8f, 8g) set. The important contributing factor is the number of g-type functions, which should be equal to 3 or larger.

Quantum Defects. Let us calculate the quantum defect curves for the first few member states of two Rydberg series, npσ and npπ, converging to $X^2\Sigma_g^+$ of a H_2^+ ion. The first three members of Rydberg series npσ are $B^1\Sigma_u^+$, $B'^1\Sigma_u^+$, and $B''^1\Sigma_u^+$, which correspond to n = 2, 3, and 4, respectively. The first two members of Rydberg series npπ are $C^1\Pi_u$ and $D^1\Pi_u$, which correspond to n = 2 and 3, respectively. Let us denote the PECs for npσ and npπ as $U_{n\mathrm{p}\sigma}(R)$ and $U_{n\mathrm{p}\pi}(R)$, respectively, and the PEC for $X^2\Sigma_g^+$ of a H_2^+ ion as $U^+(R)$. The quantum defect curves for npσ and npπ, denoted as $\mu_{\mathrm{p}\sigma}(R)$ and $\mu_{\mathrm{p}\pi}(R)$, respectively, are defined as follows:[34]

$$U_{n\mathrm{p}\sigma}(R) = U^+(R) - \frac{\mathrm{Ryd}}{[n-\mu_{\mathrm{p}\sigma}(R)]^2}$$
$$U_{n\mathrm{p}\pi}(R) = U^+(R) - \frac{\mathrm{Ryd}}{[n-\mu_{\mathrm{p}\pi}(R)]^2} \quad (2)$$

where the quantum defects are assumed to be independent of the level, *i.e.*, independent of the principal quantum number. Figure 10, which was obtained by using Eq. (2), shows that $\mu_{\mathrm{p}\pi}(R)$ is almost independent of the principal quantum number, *i.e.*, $\mu_{2\mathrm{p}\pi} \approx \mu_{3\mathrm{p}\pi}$ ($2\mathrm{p}\pi\ ^1\Pi_u \equiv C^1\Pi_u$, $3\mathrm{p}\pi\ ^1\Pi_u \equiv D^1\Pi_u$), whereas $\mu_{\mathrm{p}\sigma}(R)$ shows a small level dependence because $\mu_{3\mathrm{p}\sigma}(R)$ clearly differs from $\mu_{4\mathrm{p}\sigma}(R)$. The great departure of $\mu_{4\mathrm{p}\sigma}(R)$ from $\mu_{3\mathrm{p}\sigma}(R)$ at $R > 5.5$ a.u. is due to the perturbation by an intruder and is ignored in MQDT because it is not due to the short-range dynamics. The quantum defect for $B^1\Sigma_u^+$ also need not be considered because B is not a Rydberg state. Mulliken classified this state as semi-Rydberg.[33,35,36] Note that the behavior of the quantum defects for B is not "promoted" as $R \to \infty$, but the values of quantum defects for B' and B'' are "promoted" by 1 as $R \to \infty$. According to Mulliken, promotion may be understood by examining the correlation diagram between the combined atom limits and the separate atom limits.

Figure 10 shows that the quantum defects are sensitive to the accuracy of the calculated PECs, as evident from Eq. (2). For example, the quantum defect curve calculated with the

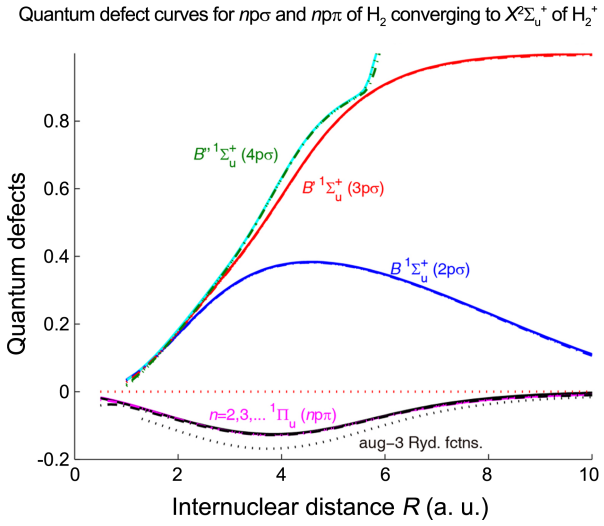

Figure 10. Quantum defect curves for the dipole-allowed states, Solid lines show those calculated for the accurate potential energy curves of Staszewska and Wolniewicz. Dotted and dash-dotted lines represent those for the potentials with (3s, 3p, 3d) Rydberg functions at each nucleus and with (8s, 8p, 8d, 8f, 8g) functions at the molecular center, respectively.

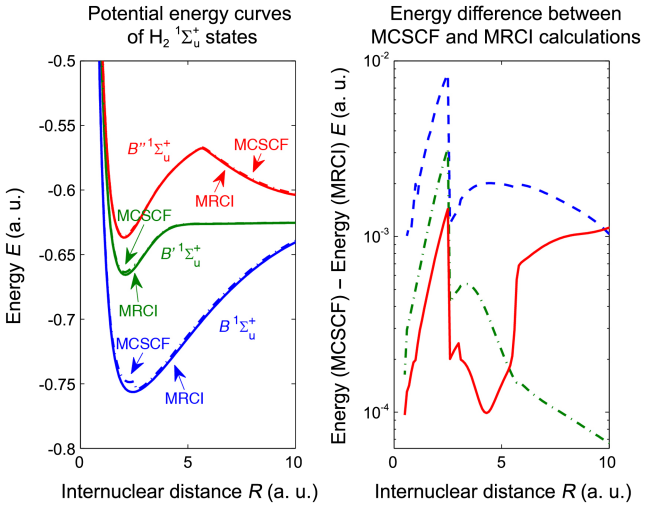

Figure 11. Potential energy curves from MCSCF and MRCI for $B,B',B''\,^1\Sigma_u^+$.

PEC obtained with (3s, 3p, 3d) Rydberg functions at each nucleus clearly differs from the accurate one. This contrasts with the quantum defect curve for the PEC with (8s, 8p, 8d) at the molecular center, which shows good agreement.

Other Methods. The hydrogen molecule is a special molecule with only two electrons. Because of this unique characteristic, various electronic structure theories yield almost the same PECs. We obtained almost the same PECs from EOM-CCSD and CASPT2 as from MRCI. Even MCSCF (or CASSCF), which yields completely different PECs for other molecules, yields almost the same PECs except for the range of small R, as shown in Figure 11. We will not explore this topic further because it is beyond the scope of this study.

Conclusion and Discussion

To calculate the photoabsorption and photoionization spectra of molecules, one needs to know the potential energy surfaces of their dipole-allowed states. In particular, the potential energy surfaces of the Rydberg states are the basic input for the calculation of photoionization by MQDT. Modern electronic structure theory is believed to be able to calculate the potential energy surfaces for the excited states, including the Rydberg states, with chemical accuracy.

Because the MRCI method is known to always yield reliable PECs, it was chosen in this study, with application to other molecules in mind. However, MRCI is not a black box method. One must provide many parameters to obtain reliable PECs. To master all the skills for obtaining potentials with chemical accuracy, we must have a system for which accurate potentials are available. The hydrogen molecule is such a system; James Coolidge–type calculations, including r_{12} variables, are available, including those for highly excited states.

Among the states that decompose into H(1s) + H(1s) and H(1s) + H(2l), the first states in their own symmetry, such as $X^1\Sigma_g^+$, $b^3\Sigma_u^+$, $B^1\Sigma_u^+$, and $a^3\Sigma_g^+$, as well as $C^1\Pi_u$ and $E,F^1\Sigma_g^+$, are considered for the calculation of PECs by the MRCI method with AVQZ in the CAS composed of $(3\sigma_g^+,1\pi_u,3\sigma_u^+,1\pi_g)$. Most of the PECS showed excellent agreement with the corresponding accurate PECs of Kolos, Wolniewicz, and their collaborators, except for $a^3\Sigma_g^+$ and $E,F^1\Sigma_g^+$. The disagreement between the two PECs in the $E,F^1\Sigma_g^+$ state is removed by increasing the size of the basis set from AVQZ to AV6Z. On the other hand, the difference for the $a^3\Sigma_g^+$ state is removed by adding the high-angular-momentum Rydberg basis functions as high as $l = 4$.

Next, the PECs for the dipole-allowed states $B^1\Sigma_u^+$, $B'^1\Sigma_u^+$, $B''^1\Sigma_u^+$, $C^1\Pi_u$, and $D^1\Pi_u$ are considered. Although the PEC for $B^1\Sigma_u^+$ can be made to agree with that of Staszewska and Wolniewicz[11] by extrapolating to the CBS limit, that for $B'^1\Sigma_u^+$ cannot be made to agree with that of Staszewska and Wolniewicz[11] even at the CBS limit. For $B''^1\Sigma_u^+$, the MRCI method fails completely with the basis set aug-cc-pVXZ. The situation is even worse for the states of $^1\Pi_u$ symmetry. The failure is due to the inadequacy of the basis set aug-ccPVXZ (X = D, T, Q, 5, 6) for the representation of Rydberg states.

Kaufmann devised a method for obtaining universal Gaussian orbital exponents that can be used to handle the Rydberg states for any neutral molecule. With the basis set augmented with Kaufmann's Rydberg functions for each atom, very excellent PECs are obtained for the states belonging to the symmetry $^1\Sigma_u^+$. Similarly, an excellent PEC is obtained for the first state of symmetry $^1\Pi_u$ with the basis set augmented with Rydberg basis functions for each atom. However, the error in the PEC compared to the accurate PEC for $D^1\Pi_u$ is larger than 10^{-3} a.u. at $0 < R < 5.5$ a.u. and appears problematic because the range of bad behavior is a physically important range.

When Rydberg basis functions located at the molecular center of charge are added, the problem of the PEC for $D^1\Pi_u$ at $0 < R < 5.5$ a.u. disappears, although a new problem arises at large R. That is, the PEC begins to deviate increasingly from the correct PEC as the internuclear distance increases. This behavior also holds for $C^1\Pi_u$. The deviation at large R occurs because the electronic state becomes more anisotropic as R becomes large, so it cannot be represented in terms of basis functions of the s, p, and d types only. The deviation disappears with the inclusion of f and g Rydberg basis functions.

Acknowledgments. This study was supported by the Basic Science Research Program through the National Research Foundation of Korea (NRF) funded by the Ministry of Education, Science, and Technology (2011-0024808).

References

1. Lee, C. W. *Bull. Korean Chem. Soc.* **2012**, *33*, 2657.
2. Lefebvre-Brion, H.; Field, R. W. *The Spectra and Dynamics of Diatomic Molecules*; Rev. and enlarged ed.; Elsevier Academic Press: Amsterdam, Boston, 2004.
3. Kolos, W.; Wolniewicz, L. *J. Chem. Phys.* **1965**, *43*, 2429.
4. Kolos, W.; Wolniewicz, L. *J. Chem. Phys.* **1966**, *45*, 509.

5. Kolos, W.; Wolniewicz, L. *J. Chem. Phys.* **1968**, *48*, 3672.
6. Kolos, W.; Wolniewicz, L. *J. Chem. Phys.* **1969**, *50*, 3228.
7. Kolos, W.; Rychlewski, J. *J. Mol. Spectrosc.* **1976**, *62*, 109.
8. Kolos, W. *J. Mol. Spectrosc.* **1976**, *62*, 429.
9. Kolos, W.; Rychlewski, J. *J. Mol. Spectrosc.* **1977**, *66*, 428.
10. Wolniewicz, L.; Dressler, K. *J. Chem. Phys.* **1988**, *88*, 3861.
11. Staszewska, G.; Wolniewicz, L. *J. Mol. Spectrosc.* **2002**, *212*, 208.
12. Wolniewicz, L.; Staszewska, G. *J. Mol. Spectrosc.* **2003**, *220*, 45.
13. Werner, H.-J.; Knowles, P. J. *J. Chem. Phys.* **1988**, *89*, 5803.
14. Andersson, K.; Malmqvist, P. Å.; Roos, B. O. *J. Chem. Phys.* **1992**, *96*, 1218.
15. Stanton, J. F.; Bartlett, R. J. *J. Chem. Phys.* **1993**, *98*, 7029.
16. Werner, H.-J.; Knowles, P. J. *J. Chem. Phys.* **1985**, *82*, 5053.
17. Knowles, P.; Werner, H.-J. *Theoret. Chim. Acta* **1992**, *84*, 95.
18. Werner, H.-J. *Adv. Chem. Phys.* **1987**, *69*, 1.
19. Dunning Jr., T. H.; Hay, P. J. In *Methods of Electronic Structure Theory*; Schaefer III, H. F., Ed.; Plenum Press: New York, 1977; Vol. 2, p 1.
20. Roos, B. O.; Andersson, K.; Fülscher, M. P.; Malmqvist, P. Å.; Serrano-Andrés, L.; Pierloot, K.; Merchán, M. In *Adv. Chem. Phys.*; John Wiley & Sons, Inc.: 1996; p 219.
21. Kaufmann, K.; Baumeister, W.; Jungen, M. *J. Phys. B* **1989**, *22*, 2223.
22. MOLPRO, version 2012.1, a package of *ab initio* programs, Werner, H.-J.; Knowles, P. J.; Knizia, G.; Manby, F. R.; Schutz, M.; others; see http://www.molpro.net.
23. Werner, H.-J.; Meyer, W. *J. Chem. Phys.* **1980**, *73*, 2342.
24. Werner, H.-J.; Reinsch, E.-A. *J. Chem. Phys.* **1982**, *76*, 3144.
25. Roos, B. *Chem. Phys. Lett.* **1972**, *15*, 153.
26. Dunning, T. H. *J. Chem. Phys.* **1989**, *90*, 1007.
27. Knowles, P. J.; Werner, H.-J. *Chem. Phys. Lett.* **1988**, *145*, 514.
28. Werner, H.-J.; Meyer, W. *J. Chem. Phys.* **1981**, *74*, 5794.
29. Hazi, A. U.; Rice, S. A. *J. Chem. Phys.* **1967**, *47*, 1125.
30. Lefebvre-Brion, H.; Moser, C. M. *J. Chem. Phys.* **1965**, *43*, 1394.
31. Hochlaf, M.; Ndome, H.; Hammoutène, D.; Vervloet, M. *J. Phys. B* **2010**, *43*, 245101.
32. Andersson, K.; Malmqvist, P. Å.; Roos, B. O.; Sadlej, A. J.; Wolinski, K. *J. Phys. Chem.* **1990**, *94*, 5483.
33. Mulliken, R. S. *Acc. Chem. Res.* **1976**, *9*, 7.
34. Atabek, O.; Dill, D.; Jungen, C. *Phys. Rev. Lett.* **1974**, *33*, 123.
35. Mulliken, R. S. *J. Am. Chem. Soc.* **1964**, *86*, 3183.
36. Mulliken, R. S. *J. Am. Chem. Soc.* **1966**, *88*, 1849.